Biochemistry and Biophysics Reports 7 (2016) 33–38

Contents lists available at ScienceDirect

Biochemistry and Biophysics Reports

journal homepage: www.elsevier.com/locate/bbrep

Partial contribution of mitochondrial permeability transition to *t*-butyl hydroperoxide-induced cell death

Xiaolei Shi, Hikaru Osaki, Yoshihiro Matsunomoto, Chisako Fujita, Daisuke Shinohe, Naoko Ashida, Hyunjin Choi, Yoshihiro Ohta *

Division of Biotechnology and Life Sciences, Institute of Engineering, Tokyo University of Agriculture and Technology, Nakacho 2-24-16, Koganei, Tokyo 184-8588, Japan

ARTICLE INFO

Article history:
Received 9 September 2015
Received in revised form
2 May 2016
Accepted 6 May 2016
Available online 9 May 2016

Keywords:
Cell death
Mitochondria
Mitochondrial permeability transition pore
Oxidative stress
t-butyl hydroperoxide

ABSTRACT

Mitochondrial permeability transition (MPT) is thought to determine cell death under oxidative stress. However, MPT inhibitors only partially suppress oxidative stress-induced cell death. Here, we demonstrate that cells in which MPT is inhibited undergo cell death under oxidative stress. When C6 cells were exposed to 250 μM *t*-butyl hydroperoxide (*t*-BuOOH), the loss of a membrane potential-sensitive dye (tetramethylrhodamine ethyl ester, TMRE) from mitochondria was observed, indicating mitochondrial depolarization leading to cell death. The fluorescence of calcein entrapped in mitochondria prior to addition of *t*-BuOOH was significantly decreased to 70% after mitochondrial depolarization. Cyclosporin A suppressed the decrease in mitochondrial calcein fluorescence, but not mitochondrial depolarization. These results show that *t*-BuOOH induced cell death even when it did not induce MPT. Prior to MPT, lactate production and respiration were hampered. Taken together, these data indicate that the decreased turnover rate of glycolysis and mitochondrial respiration may be as vital as MPT for cell death induced under moderate oxidative stress.

1. Introduction

Mitochondria utilize the pH gradients and membrane potentials that exist across their inner membranes to transport charged molecules and ions. To maintain the pH gradients and membrane potentials, it is necessary for the permeability of the inner mitochondrial membrane to be kept low. However, when mitochondria undergo Ca^{2+} overloading or oxidative stress, the inner membranes become permeable to solutes with molecular masses that are below approximately 1.5 kDa; this is known as mitochondrial permeability transition, MPT) [1]. Therefore, upon MPT, mitochondrial function changes drastically, and the intracellular environment is altered. As such, MPT is thought to be involved in cellular damage [2,3] or intracellular signal transduction [4,5]. MPT can be blocked when the mitochondrial peptidylprolyl cis-trans isomerase (PPIase) cyclophilin D is inhibited [6] or its gene is ablated [7,8], thus indicating that MPT is a protein-dependent process.

Cellular dysfunction due to reactive oxygen species (ROS) has been observed in diseases including ischemia reperfusion injury and neurodegenerative disorders [9]. ROS suppress energy production by hampering glycolysis [10,11] and mitochondrial function [12–16]. In particular, intensive studies on ROS-induced MPT have demonstrated that MPT inhibition by cyclosporin A (CsA) increases cells viability under oxidative stress. However, CsA only partially suppresses ROS-induced cell death [17,18]. In these cases, it is unclear whether cell death is accompanied by MPT or not.

To detect MPT in cells, we can monitor the translocation of small molecules across the inner membrane by using hydrophilic fluorescent dye calcein [13,14] or radiolabeled 2-deoxyglucose [15,16]; these are smaller than the MPT cutoff size of 1.5 kDa. Although calcein is suitable for simultaneous measurements of mitochondrial membrane potential and the occurrence of MPT, we must consider the effects of ROS on the mitochondrial uptake of calcein AM and the quenching of calcein fluorescence in mitochondria. In this study, we successfully excluded these effects of ROS and demonstrated that mitochondria became depolarized by

Abbreviations: AM, acetoxymethyl ester; CsA, cyclosporin A; DMEM, Dulbecco's modified Eagle's medium; $\Delta\Psi m$, mitochondrial membrane potential; FBS, fetal bovine serum; HBS, HEPES-buffered saline; MPT, mitochondrial permeability transition; *t*-BuOOH, *t*-butyl hydroperoxide; TMRE, tetramethylrhodamine ethyl ester; PPIase, peptidylprolyl cis-trans isomerase; ROS, reactive oxygen species

* Corresponding author.
E-mail address: ohta@cc.tuat.ac.jp (Y. Ohta).

http://dx.doi.org/10.1016/j.bbrep.2016.05.005

ROS even when MPT was inhibited by CsA. This result implies that ROS significantly decreases ATP production even when MPT does not occur and further promotes necrotic cell death.

2. Experimental procedures

2.1. Reagents

Calcein AM was purchased from Dojindo Laboratories (Kumamoto, Japan). Tetramethylrhodamine ethyl ester (TMRE) was purchased from Invitrogen Corporation (Carlsbad, CA). CsA and digitonin were obtained from Sigma-Aldrich Co. (St. Louis, MO). All other high purity chemicals were commercially available.

2.2. Cell Cultures

C6 glioma cell lines overexpressing wild-type or PPIase-deficient mutants (R97A) of cyclophilin D and control cells transfected with the corresponding empty vector were obtained, as described previously [19]. The cells were cultured in Dulbecco's modified Eagle's medium (DMEM) supplemented with 10% fetal bovine serum (FBS) and 100 μg/mL of geneticin in a humidified incubator at 37 °C and 5% CO_2. After enzymatic dissociation with trypsin, cells were plated in culture dishes (diameter, 35 mm) at a concentration of 2.8×10^4 cells/cm^2. The cells were cultured under the above conditions for 2 days prior to measurements.

2.3. Fluorescence staining and the addition of t-BuOOH

In order to observe the changes in the plasma membrane integrity and $\Delta\Psi$m by exposing cells to *t*-BuOOH, C6 glioma cells were loaded with 1 μM calcein AM [20] and 100 nM TMRE [21,22], respectively, for 30 min in DMEM without serum at 37 °C. Cells were then washed with DMEM and incubated with 250 μM *t*-BuOOH [13,23] in DMEM with 100 nM TMRE and 10% FBS. Immediately before microscopic observation, the medium was replaced with HEPES-buffered saline (HBS) (10 mM HEPES, 120 mM NaCl, 4 mM KCl, 0.5 mM $MgSO_4$, 1 mM NaH_2PO_4, 4 mM $NaHCO_3$, 25 mM glucose, 0.1% bovine serum albumin, pH 7.4) with 1.2 mM $CaCl_2$ and 100 nM TMRE.

In order to observe MPT in *t*-BuOOH treated cells, the calcein-digitonin technique [24] was used with slight modification. First, to trap calcein in the mitochondria, C6 glioma cells in culture dishes were incubated with 1 μM calcein AM and 100 nM TMRE for 30 min at 37 °C in DMEM with 0.005% cremophor. The calcein AM and cremophor were removed by washing cells with DMEM. The cells were then incubated with 250 μM *t*-BuOOH in DMEM with 100 nM TMRE and 10% FBS. In order to examine the effects of CsA, CsA was added to a final concentration of 5 μM after washing cells and before the addition of *t*-BuOOH, and this remained in the media throughout the remaining procedures. After the appropriate incubation time, the cells were detached from the culture dishes with 0.05% trypsin in phosphate-buffered saline (8.1 mM Na_2HPO_4, 1.5 mM KH_2PO_4, 137 mM NaCl, 2.7 mM KCl, 0.44 mM ethylenediaminetetraacetic acid, pH 7.4) with 250 μM *t*-BuOOH. After removing trypsin by centrifugation at $126 \times g$ for 10 min, the cell pellet was suspended in HBS at a density of 3×10^6 cells/mL. The suspension was divided into 3 aliquots. The first was maintained in HBS with 250 μM *t*-BuOOH (HBS(tB)). The second was incubated with 20 μM digitonin in HBS(tB) to remove the cytosolic calcein by permeabilizing the plasma membranes. The third was incubated with 100 nM TMRE in HBS(tB) to observe $\Delta\Psi$m. Immediately before microscopic observations, the cells were transferred to a hemocytometer with a 0.17-mm thick coverslip. Calcein fluorescence in the cells of the second aliquot was observed for 15–25 min after the addition of digitonin, as mitochondrial calcein fluorescence was stable during this period. After measuring the second aliquot, we measured the first and third aliquots to confirm plasma membrane integrity and the maintenance or loss of the $\Delta\Psi$m. *t*-BuOOH was added to control cells 15 min before their detachment from the dishes to compensate for the possible bleaching of calcein fluorescence. After detachment, all procedures were performed at 25 °C and completed within 30 min.

2.4. Imaging and Analysis of Calcein and TMRE Fluorescence

In order to obtain the fluorescence images, we used an inverted epifluorescence microscope (IX-70; Olympus Corporation, Tokyo, Japan). The magnification of the objective lens was 20 times (Uapo20X/340, NA = 0.75; Olympus Corporation). Calcein fluorescence was monitored using a 75-W xenon lamp through a 20-nm bandpass filter centered at 480 nm. The illumination intensity was reduced to 6% with a neutral density filter. Light emitted between 515 and 550 nm was collected with a cooled CCD camera (Sensicam QE, PCO AG; Kelheim, Germany). For the TMRE fluorescence, excitation was achieved with a 15-nm bandpass filter centered at 535 nm. Fluorescence $>$ 580 nm was collected [25,26]. The illumination intensity was reduced to 25% with a neutral density filter. All images were obtained with 2×2 binning pixels and an exposure time of 1 s. The fluorescence readouts were digitized to 12 bits and analyzed with image-processing software (MetaMorph; Molecular Devices, Inc., Sunnyvale, CA). In order to analyze the fluorescence intensity of intracellular calcein, we identified the outline of each cell in the transmitted image and obtained the average intensity of the fluorescence within the region surrounded by the outline. The background intensity of the fluorescence was obtained as the average intensity within a region where the intensity of the fluorescence was not affected by the cells stained with calcein. This was subtracted from the intensity of the calcein fluorescence in each cell.

2.5. Measurements of cell respiration

Prior to the measurements of cell respiration, cells grown in culture dishes were incubated with 250 μM *t*-BuOOH in DMEM with 10% FBS for 15 min at 37 °C. The cells were then detached from the culture dishes and collected, as described in the section on the calcein-digitonin technique. Cells not incubated with *t*-BuOOH were used as a control. During cell respiration measurements, the cells were suspended in HBS(tB) with 1.2 mM $CaCl_2$ at a concentration of 1.5×10^7 cells/mL. To evaluate cell respiration, oxygen concentrations were measured with a Clark-type oxygen electrode (Iijima-Denshi, Aichi, Japan) for 10 min at 37 °C. These measurements were completed within 40 min after the addition of *t*-BuOOH to cells grown in culture dishes.

2.6. Measurements of ATP and lactate production

Prior to determination of lactate levels, cells were incubated in DMEM without FBS for 20 min. When rotenone and/or *t*-BuOOH were added, these reagents were present during this incubation. Cells were then washed twice with DMEM without FBS and were incubated in the medium for 30 min in the presence or absence of 600 nM rotenone and/or 250 μM *t*-BuOOH. After this incubation, lactate in the medium was determined enzymatically by a test kit (L-lactic acid, Boehringer Mannheim, Germany). The amount of cells in a dish was determined as protein amount using a protein assay with BSA as a standard.

For determination of ATP, cells were plated in 96-well microplates at a concentration of 2500 cells/well and cultured in DMEM with 10% FBS for 48 h at 37 °C in a CO_2 incubator. When *t*-BuOOH

was added, cells were incubated with 250 μM *t*-BuOOH in DMEM with 10% FBS for 30 min. ATP content was determined with a commercial kit (CellTiter-Glo® Luminescent Cell Viability Assay, Promega, WI, USA). The amount of cells per well was determined as protein amount using a protein assay with BSA as a standard.

2.7. Statistical analysis

We averaged the data from at least three independent experiments. The results were expressed as mean ± SEM, and they were analyzed by ANOVA followed by the Student-Newman-Keuls test. Differences were considered statistically significant with P values less than 0.05.

3. Results and discussion

3.1. Microscopic observation of the cellular responses following *t*-BuOOH treatment

To examine the responses of C6 glioma cells to *t*-BuOOH, we observed the changes in cellular morphology, plasma membrane integrity, and ΔΨm after addition of *t*-BuOOH. The results are shown in Fig. 1.

Initially, we observed the C6 glioma cells transfected with the empty vector (vector control cells). After incubation for 60 min with 250 μM *t*-BuOOH, the cells showed shrinkage and blebbing. The plasma membrane integrity and ΔΨm appeared to be unchanged. After incubation for 150 min, the ΔΨm had significantly dissipated as indicated by the decrease in the intensity of the TMRE fluorescence in the cells. The incubation time of the cells with *t*-BuOOH until the ΔΨm dissipated significantly depended on the preparations and ranged from 150 to 180 min. In the early stages after the depolarization of mitochondria (Fig. 1(A), 150 min), the plasma membranes of the cells did not rupture as the calcein fluorescence in the cells was unchanged. The plasma membranes ruptured 30–40 min following mitochondrial depolarization, as indicated by the release of cytosolic calcein and drastic changes in cellular morphology (Fig. 1(A), 210 min). The dissipation of ΔΨm before the rupture of the plasma membranes was consistent with that reported in previous studies [13,27]. In the present study, we defined cell death as plasma membrane rupture.

The cellular response to 250 μM *t*-BuOOH was accelerated when wild-type of cyclophilin D was overexpressed (Fig. 1(B)). On the contrary, when the PPIase activity of cyclophilin D was inhibited (Fig. 1(C) and (D)), the progression of the responses was not significantly changed. In spite of the PPIase activity of cyclophilin D, almost all cells examined initially exhibited shrinkage and blebbing, then the disruption of ΔΨm, and finally plasma membrane rupture when *t*-BuOOH was added at 250 μM. In contrast, when the *t*-BuOOH concentration was decreased to 50 μM, inhibition of cyclophilin D suppressed all features observed in the presence of 250 μM *t*-BuOOH (data not shown). These results suggest that 250 μM *t*-BuOOH induces cell death by

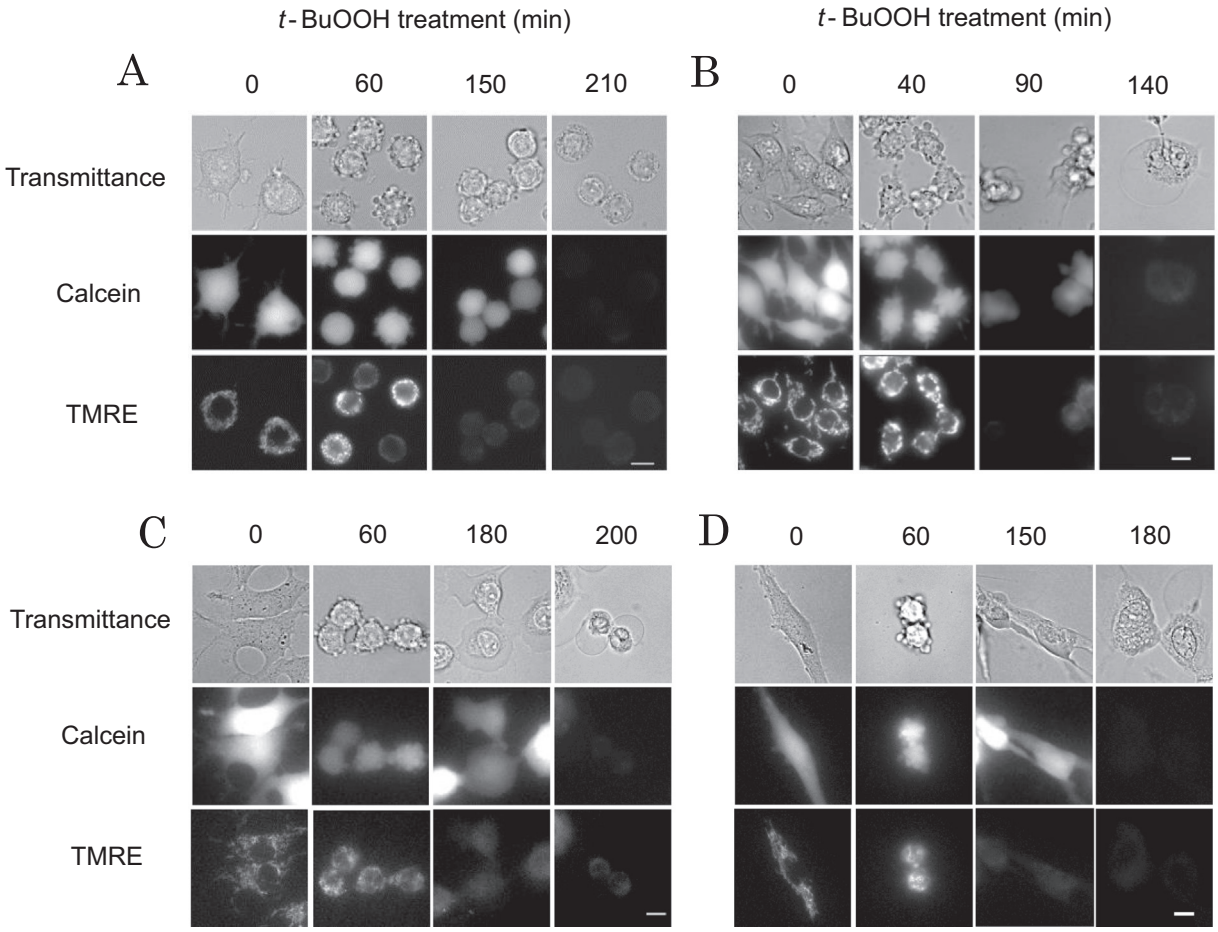

Fig. 1. Effects of *t*-BuOOH on cell morphology, plasma membrane integrity, and ΔΨm. Cells were stained with calcein in order to examine the integrity of the plasma membranes and with TMRE in order to observe the ΔΨm. Bar, 10 μm. At t =0 min, 250 μM *t*-BuOOH was added to the cells. A) Vector control. B) C6 glioma cells overexpressing wild-type of cyclophilin D. C) C6 glioma cells overexpressing PPIase-deficient mutants (R97A) of cyclophilin D. D) Vector control cells in the presence of 5 μM CsA.

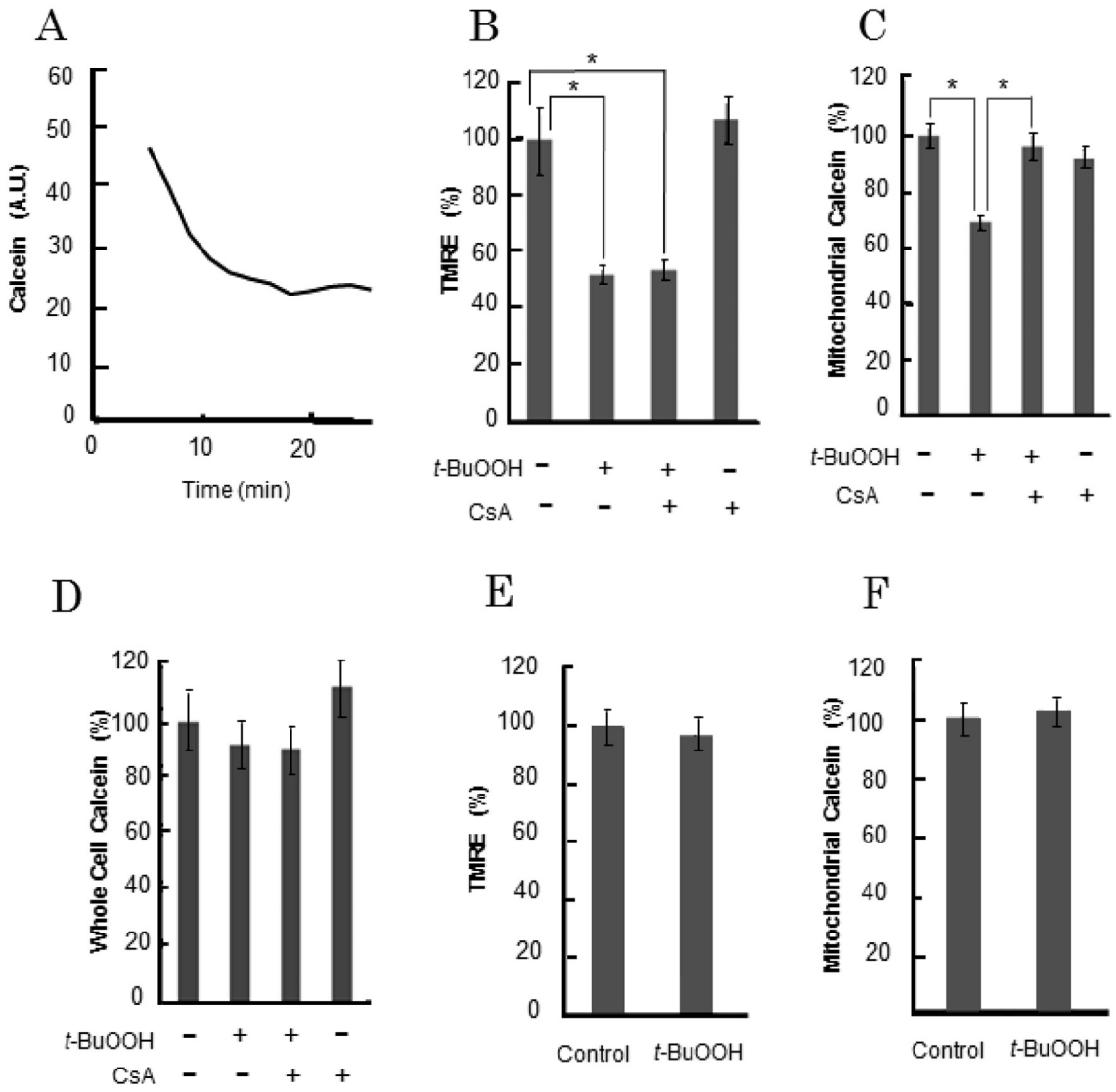

Fig. 2. Analysis of calcein and TMRE fluorescence before plasma membrane rupture. Vector control cells were exposed to *t*-BuOOH for 150 min (A–D) or 90 min (E, F). (A) Time course of changes in calcein fluorescence in cells after addition of digitonin. At t=0, digitonin was added to cells. The cells were then transferred to a microscope stage. (B) TMRE fluorescence in cells. (C) Mitochondrial calcein fluorescence in cells. (D) Calcein fluorescence in intact cells without digitonin treatment. (E) TMRE fluorescence before dissipation of the ΔΨm. (F) Mitochondrial calcein fluorescence in cells before ΔΨm dissipation. (B–F) The average intensity of the fluorescence of control cells without *t*-BuOOH and CsA treatment was adjusted to 100, and results expressed as a represent means ± SE (n=4). *, $P < 0.05$ vs. control.

mechanisms additional to those by which 50 μM *t*-BuOOH induces cell death.

3.2. Detection of MPT with the calcein-digitonin technique

MPT occurs in cells during oxidative stress, leading to cell death [13]. Although CsA is a MPT inhibitor, our results show that 250 μM *t*-BuOOH induces cell death in the presence of CsA. Therefore, we examined whether 250 μM *t*-BuOOH induced MPT in cells in the presence of CsA. For this purpose, C6 glioma cells (vector control) were analyzed using the calcein-digitonin technique prior to plasma membrane rupture. In all cells examined after the digitonin mediated plasma membrane permeabilization, intracellular calcein fluorescence was largely decreased to 5–10% due to the release of calcein from the cytosol to the medium. This indicates that calcein was mainly distributed in the cytosol prior to the addition of digitonin, and that it was therefore impossible to identify mitochondrial calcein fluorescence for the first minutes after digitonin treatment (Fig. 2(A)). After the release of cytosolic calcein, calcein fluorescence in the cells became stable, regardless of the incubation with *t*-BuOOH. During the stable phase, most of the residual calcein fluorescence was localized to the mitochondria as reported previously [24]. Therefore, we measured cellular calcein fluorescence during the stable phase as representative of mitochondrial calcein fluorescence.

We measured the mitochondrial calcein fluorescence after ΔΨm dissipation induced by *t*-BuOOH, since MPT should accompany the collapse of the ΔΨm. After ΔΨm dissipation, the calcein fluorescence in the mitochondria of digitonin-permeabilized cells decreased to approximately 70% of control levels (Fig. 2(B) and (C)); however, the calcein fluorescence in a whole cell remained unchanged after ΔΨm dissipation (Fig. 2(D)). After observing mitochondrial calcein with the calcein-digitonin technique, we confirmed that the plasma membranes did not rupture when digitonin was absent. However, when ΔΨm was maintained, *t*-BuOOH did not decrease mitochondrial calcein (Fig. 2(E) and (F)). These results suggest that *t*-BuOOH induced MPT in the intact cells before plasma membrane rupture, and that the effects of *t*-BuOOH

on mitochondrial uptake of calcein AM and the quenching of calcein fluorescence in mitochondria were negligible under the present condition.

Next, we examined the effects of CsA on mitochondrial calcein fluorescence after the dissipation of $\Delta\Psi$m. For this, we added CsA to the cells that had been washed with HBS following incubation with calcein AM. This removal of calcein AM from the medium helped to suppress the CsA-induced increase in calcein fluorescence in a whole cell (Fig. 2(D)), as CsA inhibits the multidrug resistance P-glycoprotein that carries calcein AM out of the cells [28,29]. In the presence of *t*-BuOOH, CsA inhibited the decrease in mitochondrial calcein fluorescence after dissipation of $\Delta\Psi$m, while CsA alone did not affect the mitochondrial calcein fluorescence (Fig. 2(C)). These findings indicate that CsA inhibited MPT induced by *t*-BuOOH at 250 μM in intact cells.

In the above experiments, we exclusively measured vector control cells and induced MPT with 250 μM *t*-BuOOH. To detect the occurrence of MPT with the calcein-digitonin technique, it is necessary to obtain the cell population in which the majority of cells possess depolarized mitochondria and intact plasma membranes. To achieve this, we used 250 μM *t*-BuOOH. In contrast, in the presence of 50 μM *t*-BuOOH, the cell population contained cells at various stages of the *t*-BuOOH response, since the rate of progression of the response depended significantly on individual cells. The concentration of *t*-BuOOH used here (250 μM) is adequate to examine the molecular mechanisms in response to oxidative stress, because the concentration of *t*-BuOOH is similar to those used in the previous studies [30,31]. In addition, calcein distribution in cells were affected by expression of cyclophilin D (Shinohe, unpublished results). Therefore, we exclusively measured the mitochondrial calcein in vector control cells and did not compare the residual calcein in mitochondria among C6 glioma cell lines overexpressing wild-type, PPIase-deficient mutants (R97A) of cyclophilin D, and the vector control.

3.3. *Effects of t-BuOOH on cells before dissipation of $\Delta\Psi$m*

In spite of MPT suppression by CsA, *t*-BuOOH induced cell death at 250 μM, as shown by plasma membrane rupture. These results indicate that there are mechanisms other than MPT by which *t*-BuOOH induces cell death. This interpretation is consistent with previous studies showing that CsA only partially suppresses ROS-induced cell death [17,18]. Since the decrease in intracellular ATP concentration occurs during oxidative stress [10,32], and ATP depletion in cells can lead to the collapse of cell homeostasis, resulting in cell death [11,33], we measured the effect of *t*-BuOOH on cellular ATP concentration before the occurrence of MPT. As shown in Fig. 3(A), *t*-BuOOH significantly decreased ATP concentration in the cells at 250 μM.

In order to examine the mechanism by which *t*-BuOOH decreases ATP concentration in cells without MPT, we measured the effects of *t*-BuOOH on two major ATP-generating systems, glycolysis and oxidative phosphorylation. *t*-BuOOH significantly decreased lactate production at 250 μM (Fig. 3(B)). The decrease in lactate production was also observed in the presence of rotenone. These results indicate that the glycolytic flux rate was depressed by *t*-BuOOH. The observed depression of the glycolytic flux rate is consistent with the previous observation that GAPDH involved in glycolysis was specifically inactivated during oxidative stress [10,32]. Next, in order to examine the effects of *t*-BuOOH on oxidative phosphorylation, we measured the respiration rate (Fig. 3(C)). *t*-BuOOH significantly increased the cell respiration rate in the presence of 5 μM oligomycin (V_2), although it had no effects on the respiration rate in the absence of oligomycin (V_1) (Fig. 3(D)). To confirm the stimulation of V_2 by *t*-BuOOH, we calculated the ratio (V_2/V_1) in order to compensate for the slight differences in the

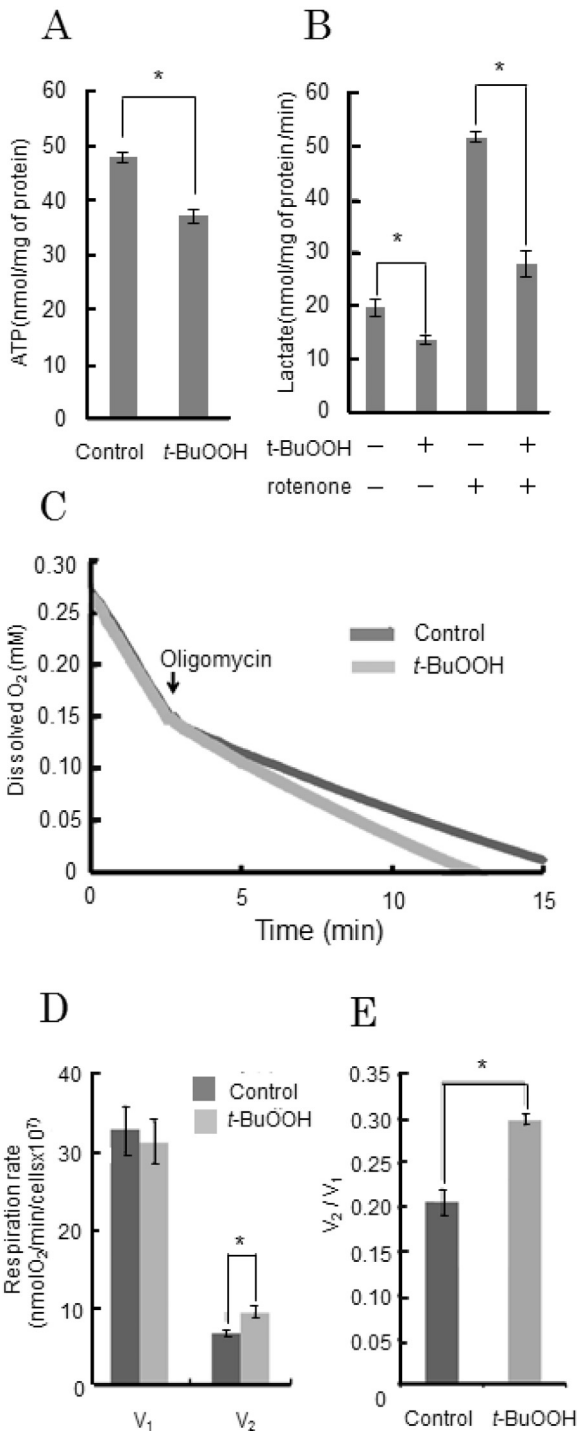

Fig. 3. Effects of *t*-BuOOH on energy metabolism of vector control cells. *t*-BuOOH was added to culture medium to a final concentration of 250 μM. (A) Intracellular ATP level and (B) lactate production of vector control cells. (C) Changes in oxygen concentration in the cell suspension. At t=0, cells were added to the buffer. The arrow marks the addition of 5 μM oligomycin to the cell suspension. (D) Respiration rates in the absence of oligomycin (V_1) and in the presence of oligomycin (V_2). (E) Effects of *t*-BuOOH on the ratio of respiration rate (V_2/V_1). Results represent means ± SE (n=3 for A and n=5 for (B, D, and E)). *, $P < 0.05$ vs. control.

number of cells among the preparations, as the respiration rate depends on the cell number. The presence of *t*-BuOOH significantly increased the ratio from 0.21 to 0.30 (Fig. 3(E)), suggesting that uncoupling of oxidative phosphorylation was stimulated by the presence of *t*-BuOOH. *t*-BuOOH did not decrease basal respiration, probably because the increase in respiration caused by

uncoupling of oxidative phosphorylation compensated for the decrease in respiration by the reduction in the supply of pyruvate.

Although it is unclear whether 250 μM *t*-BuOOH dissipated the ΔΨm by MPT in the absence of CsA, we think that MPT induced the ΔΨm dissipation, as MPT is more sensitive to *t*-BuOOH than the inhibition of glycolysis and the induction of uncoupling of oxidative phosphorylation. This idea is supported by the fact that the inhibition of MPT by CsA suppresses cell death when *t*-BuOOH is added at a lower concentration, and by the fact that the significant decrease in calcein fluorescence in mitochondria is observed only after dissipation of ΔΨm. However, the difference in the time between ΔΨm dissipation by MPT and that by the non-MPT mechanism is likely to be small under these conditions.

4. Conclusions

When the concentration of *t*-BuOOH was low (50 μM), the main factor inducing the cell death was MPT. When the concentration of *t*-BuOOH increased to 250 μM, *t*-BuOOH induced cell death by both MPT dependent and independent mechanisms. Mechanisms other than MPT included uncoupling of oxidative phosphorylation and inhibition of glycolysis, both of which lead to a decrease in intracellular ATP concentration that can induce necrosis [11,33]. These results indicate that MPT is not the sole reason for the *t*-BuOOH-induced cell death and that MPT only partially contributes to cell death induced by 250μM *t*-BuOOH.

Acknowledgments

This work was supported in part by a Grant-in-Aid for Scientific Research (C) No. 25440065 from the Japan Society for the Promotion of Science (JSPS) No. 25440065. We appreciate Drs. H. Osada and K. Machida (RIKEN) for kind a supply of the vector CypD.

Appendix A. Transparency document

Transparency document associated with this article can be found in the online version at http://dx.doi.org/10.1016/j.bbrep.2016.05.005.

References

[1] R.A. Haworth, D.R. Hunter, The Ca^{2+}-induced membrane transition in mitochondria. II. Nature of the Ca2+ trigger site, Arch. Biochem. Biophys. 195 (1979) 460–467.
[2] M.E. Soriano, L. Nicolosi, P. Bernardi, Desensitization of the permeability transition pore by cyclosporin a prevents activation of the mitochondrial apoptotic pathway and liver damage by tumor necrosis factor-alpha, J. Biol. Chem. 279 (2004) 36803–36808.
[3] H. Du, L. Guo, S. Yan, A.A. Sosunov, G.M. McKhann, S.S. Yan, Early deficits in synaptic mitochondria in an Alzheimer's disease mouse model, PNAS 107 (2010) 18670–18675.
[4] F. Ichas, L.S. Jouaville, J.P. Mazat, Mitochondria are excitable organelles capable of generating and conveying electrical and calcium signals, Cell 89 (1997) 1145–1153.
[5] Q. Ma, H. Fang, W. Shang, L. Liu, Z. Xu, T. Ye, X. Wang, M. Zheng, Q. Chen, H. Cheng, Superoxide flashes: early mitochondrial signals for oxidative stress-induced apoptosis, J. Biol. Chem. 286 (2011) 27573–27581.
[6] A.P. Halestrap, A.M. Davidson, Inhibition of Ca^{2+}-induced large-amplitude swelling of liver and heart mitochondria by cyclosporin is probably caused by the inhibitor binding to mitochondrial-matrix peptidyl-prolyl cis-trans isomerase and preventing it interacting with the adenine nucleotide translocase, Biochem. J. 268 (1990) 153–160.
[7] C.P. Baines, R.A. Kaiser, N.H. Purcell, N.S. Blair, H. Osinska, M.A. Hambleton, E. W. Brunskill, M.R. Sayen, R.A. Gottlieb, G.W. Dorn, J. Robbins, J.D. Molkentin, Loss of cyclophilin D reveals a critical role for mitochondrial permeability transition in cell death, Nature 434 (2005) 658–662.
[8] T. Nakagawa, S. Shimizu, T. Watanabe, O. Yamaguchi, K. Otsu, H. Yamagata, H. Inohara, T. Kubo, Y. Tsujimoto, Cyclophilin ᴅ-dependent mitochondrial permeability transition regulates some necrotic but not apoptotic cell death, Nature 434 (2005) 652–658.
[9] M. Valko, D. Leibfritz, J. Moncol, M.T. Cronin, M. Mazur, J. Telser, Free radicals and antioxidants in normal physiological functions and human disease, Int. J. Biochem. Cell Biol. 39 (2007) 44–84.
[10] P.A. Hyslop, D.B. Hinshaw, W.A. Halsey Jr, I.U. Schraufstätter, R.D. Sauerheber, R.G. Spragg, J.H. Jackson, C.G. Cochrane, Mechanisms of oxidant-mediated cell injury. The glycolytic and mitochondrial pathways of ADP phosphorylation are major intracellular targets inactivated by hydrogen peroxide, J. Biol. Chem. 263 (1988) 1665–1675.
[11] H.C. Ha, S.H. Snyder, Poly(ADP-ribose) polymerase is a mediator of necrotic cell death by ATP depletion, PNAS 96 (1999) 13978–13982.
[12] R. Imberti, A.L. Nieminen, B. Herman, J.J. Lemasters, Mitochondrial and glycolytic dysfunction in lethal injury to hepatocytes by t-butylhydroperoxide: protection by fructose, cyclosporin A and trifluoperazine, J. Pharmacol. Exp. Ther. 265 (1993) 392–400.
[13] A.L. Nieminen, A.K. Saylor, S.A. Tesfai, B. Herman, J.J. Lemasters, Contribution of the mitochondrial permeability transition to lethal injury after exposure of hepatocytes to *t*-butylhydroperoxide, Biochem. J. 307 (1995) 99–106.
[14] G. Loor, J. Kondapalli, H. Iwase, N.S. Chandel, G.B. Waypa, R.D. Guzy, T.L. Vanden Hoek, P.T. Schumacke, Mitochondrial oxidant stress triggers cell death in simulated ischemia-reperfusion, Biochim. Biophys. Acta 1813 (2011) 1382–1394.
[15] P.M. Ker, M.S. Suleiman, A.P. Halestrap, Reversal of permeability transition during recovery of hearts from ischemia and its enhancement by pyruvate, Am. J. Physiol. 276 (1999) H496–H502.
[16] K.V. Rama Rao, A.R. Jayakumar, M.D. Norenberg, Role of oxidative stress in the ammonia-induced mitochondrial permeability transition in cultured astrocytes, Neurochem. Int. 47 (2005) 31–38.
[17] K.-W. Oh, T. Qian, D.A. Brenner, J.J. Lemasters, Salicylate enhances necrosis and apoptosis mediated by the mitochondrial permeability transition, Toxicol. Sci. 73 (2003) 44–52.
[18] J.S. Kim, Y. Jin, J.J. Lemasters, Reactive oxygen species, but not Ca2+ overloading, trigger pH- and mitochondrial permeability transition-dependent death of adult rat myocytes after ischemia-reperfusion, Am. J. Physiol. Heart Circ. Physiol. 290 (2006) H2024–H2034.
[19] K. Machida, Y. Ohta, H. Osada, Suppression of apoptosis by cyclophilin D via stabilization of hexokinase II mitochondrial binding in cancer cells, J. Biol. Chem. 281 (2006) 14314–14320.
[20] N.G. Papadopoulos, G.V. Dedoussis, G. Spanakos, A.D. Gritzapis, C.N. Baxevanis, M. Papamichail, An improved fluorescence assay for the determination of lymphocyte-mediated cytotoxicity using flow cytometry, J. Immunol. Methods 177 (1994) 101–111.
[21] L.M. Loew, R.A. Tuft, W. Carrington, F.S. Fay, Imaging in five dimensions: time-dependent membrane potentials in individual mitochondria, Biophys. J. 65 (1993) 2396–2407.
[22] S. Nakayama, T. Sakuyama, S. Mitaku, Y. Ohta, Fluorescence imaging of metabolic responses in single mitochondria, Biochem. Biophys. Res. Commun. 290 (2002) 23–28.
[23] G. Petrosillo, N. Moro, F.M. Ruggiero, G. Paradies, Melatonin inhibits cardiolipin peroxidation in mitochondria and prevents the mitochondrial permeability transition and cytochrome c release, Free Radic. Biol. Med. 47 (2009) 969–974.
[24] H. Tazawa, C. Fujita, K. Machida, H. Osada, Y. Ohta, Involvement of cyclophilin D in mitochondrial permeability transition induction in intact cells, Arch. Biochem. Biophys. 481 (2009) 59–64.
[25] K. Haseda, K. Kanematsu, K. Noguchi, H. Saito, N. Umeda, Y. Ohta, Significant correlation between refractive index and activity of mitochondria: single mitochondrion study, Biomed. Opt. Express 6 (2015) 859–869.
[26] T. Shibata, S. Yamashita, K. Hirusaki, K. Katoh, Y. Ohta, Isolation of mitochondria by gentle cell membrane disruption, and their subsequent characterization, Biochem. Biophys. Res. Commun. 463 (2015) 563–568.
[27] M. Akao, B. O'Rourke, Y. Teshima, J. Seharaseyon, E. Marbán, Mechanistically distinct steps in the mitochondrial death pathway triggered by oxidative stress in cardiac myocytes, Circ. Res. 92 (2003) 186–194.
[28] M. Dietel, I. Herzig, A. Reymann, I. Brandt, B. Schaefer, A. Bunge, H. J. Heidebrecht, A. Seidel, Secondary combined resistance to the multidrug-resistance-reversing activity of cyclosporin A in the cell line F4–6RADR-CsA, J. Cancer Res. Clin. Oncol. 120 (1994) 263–271.
[29] Z. Holló, L. Homolya, C.W. Davis, B. Sarkadi, Calcein accumulation as a fluorometric functional assay of the multidrug transporter, Biochim. Biophys. Acta 1191 (1994) 384–388.
[30] M. Crompton, H. Ellinger, A. Costi, Inhibition by cyclosporin A of a Ca^{2+}-dependent pore in heart mitochondria activated by inorganic phosphate and oxidative stress, Biochem. J. 255 (1988) 357–360.
[31] L. Han, L.B. Du, A. Kumar, H.Y. Jia, X.J. Liang, Q. Tian, G.J. Nie, Y. Liu, Inhibitory effects of trolox-encapsulated chitosan nanoparticles on *tert*-butylhydroperoxide induced RAW264.7 apoptosis, Biomaterials 33 (2012) 8517–8528.
[32] Y.-J. Lee, E. Shacter, Hydrogen peroxide inhibits activation, not activity, of cellular caspase-3 in vivo, Free Radic. Biol. Med. 29 (2000) 684–692.
[33] W.-X. Zong, C.B. Thompson, Necrotic death as a cell fate, Genes Dev. 20 (2006) 1–15.